Supporting Information

Hysteresis in the thermally induced phase transition of cellulose ethers

Navid Bizmark[1,2*], *Nicholas J. Caggiano*[2†], *Jason X. Liu*[3†], *Craig B. Arnold*[2,3], *Robert K. Prud'homme*[2], *Sujit S. Datta*[2], *Rodney D. Priestley*[1,2*]

[1]Princeton Institute for the Science and Technology of Materials, Princeton University, Princeton, New Jersey 08540, United States of America

[2]Department of Chemical and Biological Engineering, Princeton University, Princeton, New Jersey 08540, United States of America

[3]Department of Mechanical and Aerospace Engineering, Princeton University, Princeton, New Jersey 08540, United States of America

*Corresponding authors: Navid Bizmark (nbizmark@princeton.edu) and Rodney D. Priestley (rpriestl@princeton.edu)

† Contributed equally.

Using the Flory-Huggins solution theory for a binary polymer-solvent system, we explain the Gibbs free energy associated with the mixing of polymer and solvent, ΔG, per unit mole of lattice sites as $\Delta G = RT\left[\frac{\phi_{\mathrm{p}}}{n}\ln\phi_{\mathrm{p}} + \left(1-\phi_{\mathrm{p}}\right)\ln\left(1-\phi_{\mathrm{p}}\right) + \phi_{\mathrm{p}}\left(1-\phi_{\mathrm{p}}\right)\chi_{\text{p-s}}\right]$, where R is the gas constant, T is temperature, ϕ_{p} is the volume fraction of polymer, n is the degree of polymerization, and $\chi_{\text{p-s}}$ is the effective polymer-solvent interaction parameter.[1,2] $\chi_{\text{p-s}}$ represents a qualitative understanding of the conditions for which the polymers are soluble in the solvent: when $\chi_{\text{p-s}} < 0$, polymer-solvent interaction is favorable, making the polymer soluble in the solvent, whereas when $\chi_{\text{p-s}} > 0$, polymer may phase separate from the solvent. While this interpretation is practically useful, previous studies have shown that $\chi_{\text{p-s}}$ remains a complex function of polymer volume fraction and temperature for thermoresponsive polymers.[1–5] Hence, we treat $\chi_{\text{p-s}}$ as an effective polymer-solvent interaction parameter addressing qualitatively the solubility state of polymer in water, which itself is a complex function of molecular-level hydrophobic interaction and hydrogen bonding as formulated in the Hansen solubility parameters.[6]

The relationship between $\chi_{\text{p-s}}$ and temperature can be theoretically expressed in a general form[7]

$$\chi_{\text{p-s}} = a + \frac{b}{T} \qquad \text{S1}$$

where a and b are temperature-independent quantities. For HPC with an endothermic de-mixing transition (see Figure 5A in the manuscript), b has a negative value, and therefore, $\chi_{\text{p-s}}$ increases at increasing temperature. Additionally, the relationship between $\chi_{\text{p-s}}$ ($\chi^{*}_{\text{p-s}}$) at which HPC droplets have been formed can be expressed as follows [7]

$$\chi^{*}_{\text{p-s}} = \frac{1}{2} + \frac{1}{\sqrt{n}} + \frac{1}{2n} \qquad \text{S2}$$

Considering Eq. S1 and S2, we expect that the LCST of low MW polymers must be higher than that of large MW polymers.

Moreover, when the temperature is further increased far above the LCST, the increase in $\chi_{\text{p-s}}$ drives the HPC droplets to expel water, transitioning to dehydrated spheres. The amount of water expulsion for large MW is more for a given $\chi_{\text{p-s}}$ as reflected in the variations in the volume fraction of polymer in the condensate ($\phi_{\mathrm{p}}^{\alpha}$) as a function of $\chi_{\text{p-s}}$ (see Figure S1 in the Supporting Information).

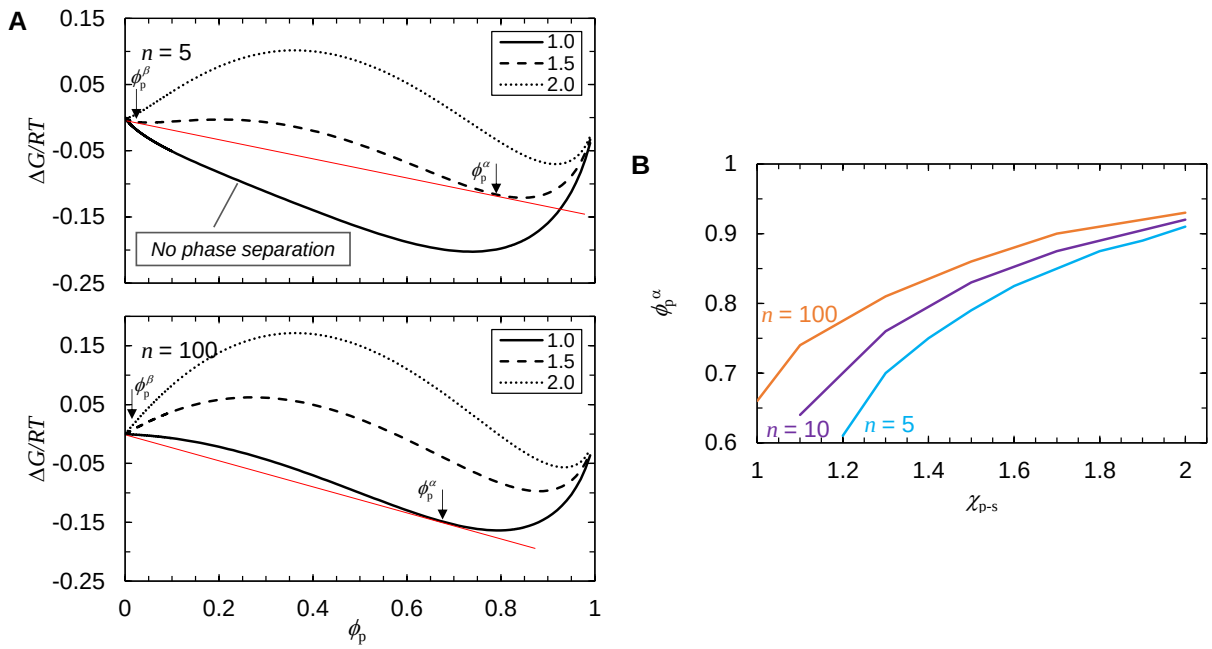

Figure S1. (A) Estimates of Gibbs free energy per unit mole of lattice sites (ΔG) for different $\chi_{\text{p-s}}$ (1.0, 1.5, and 2.0) and two different degrees of polymerization (5 and 100) as noted in the legend. The solid red line shows the two points on the curve that have a common tangent (the tie line between the two separated phases). (B) Volume fraction of polymer in the condensate phase (ϕ_{p}^{α}) as a function of $\chi_{\text{p-s}}$ for three different degrees of polymerization. For larger MW at a given $\chi_{\text{p-s}}$, the condensate phase is less hydrated as experimentally observed in Figure 3A.

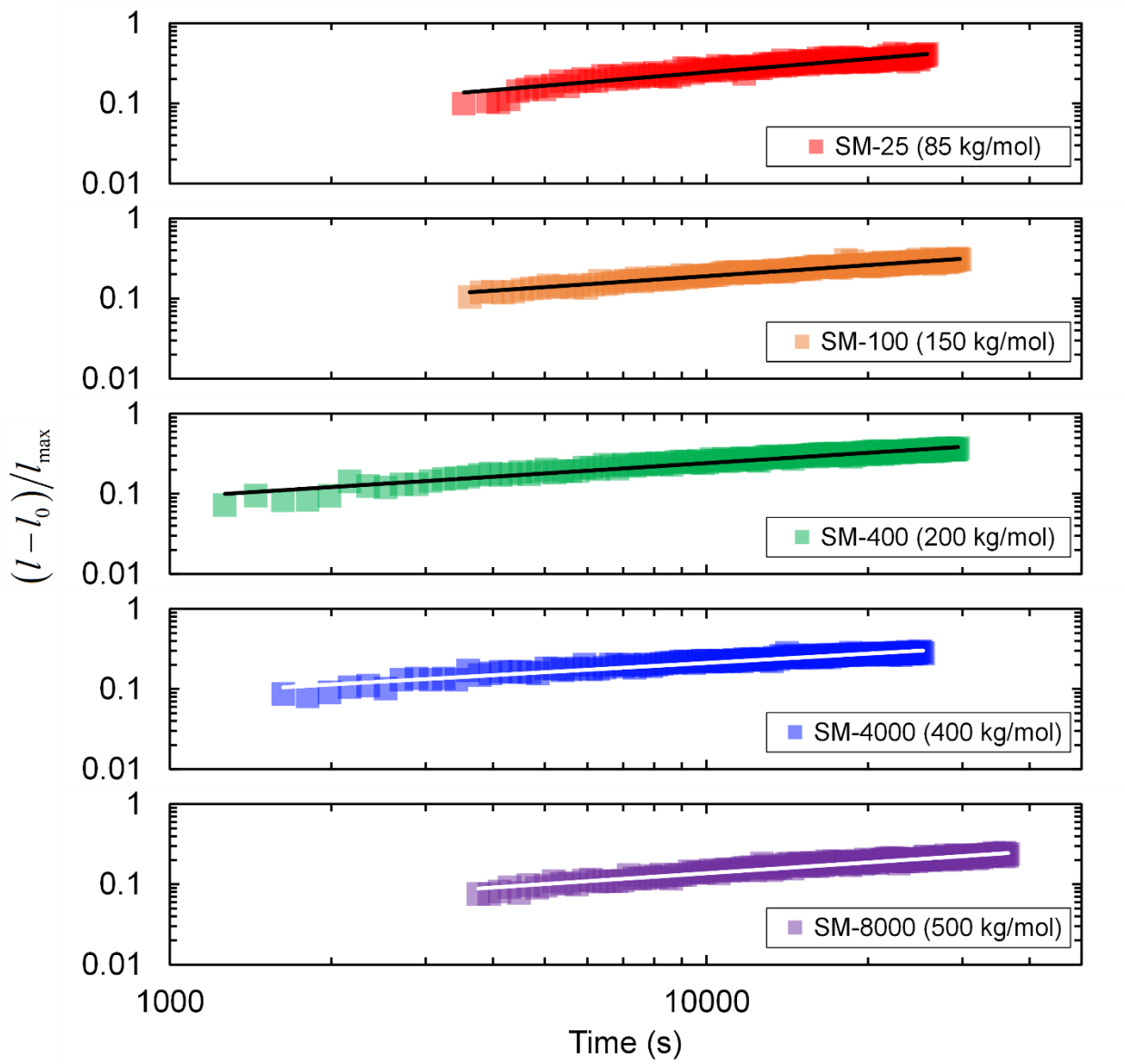

Trade name	A	B	R^2
SM-25 (85 kg/mol)	1.5×10^{-3}	0.55	0.91
SM-100 (150 kg/mol)	2.9×10^{-3}	0.45	0.96
SM-400 (200 kg/mol)	4.7×10^{-3}	0.43	0.96
SM-4000 (400 kg/mol)	6.1×10^{-3}	0.38	0.95
SM-8000 (500 kg/mol)	2.2×10^{-3}	0.45	0.95

Figure S2. The power-law fits, solid lines of $\frac{l(t)-l_0}{l_{max}} = At^B$, to the entire data sets shown in Figure 7 of the manuscript. The fitting parameters, A and B, are reported for each case.

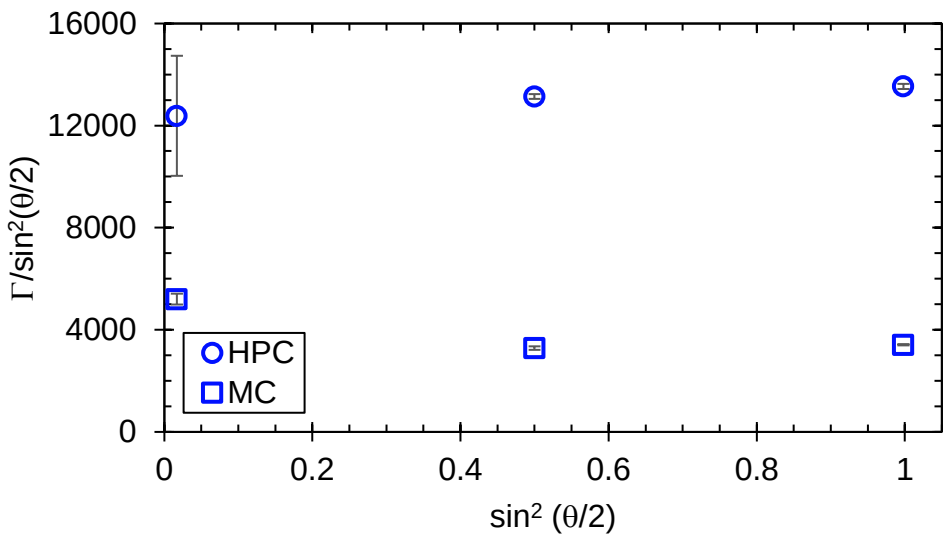

Figure S3. Angular dependency of decay rate, Γ, for HPC globules and MC fibrils at 70 °C.

We computed the decay rate, Γ, by fitting $1+a\exp(-2\Gamma\tau)$ to $g_2(\tau)=\langle I(t)I(t+\tau)\rangle/\langle I(t)\rangle^2$ as explained in the manuscript.[8] For spherical particle suspensions, $\Gamma=-Dq^2$, where D is the diffusion coefficient of particle and $q=\frac{4\pi\eta}{\lambda}\sin\left(\theta/2\right)$. Here, η and λ are the viscosity of medium and the wavelength of incident light, respectively, that have been constant during the course angular measurements. θ is the angle at which the detector has been located: 15°, 90°, and 175°. For symmetric particles, diffusion coefficient, and thus, scattered light must be similar in all directions. In contrast, diffusion coefficient for anisotropic particles varies in different direction, resulting in different angular light scattering. Therefore, the plot of $\frac{\Gamma}{\sin^2\left(\theta/2\right)}$ against $\sin^2\left(\theta/2\right)$ is expected to not vary for spherical particles but changes otherwise.

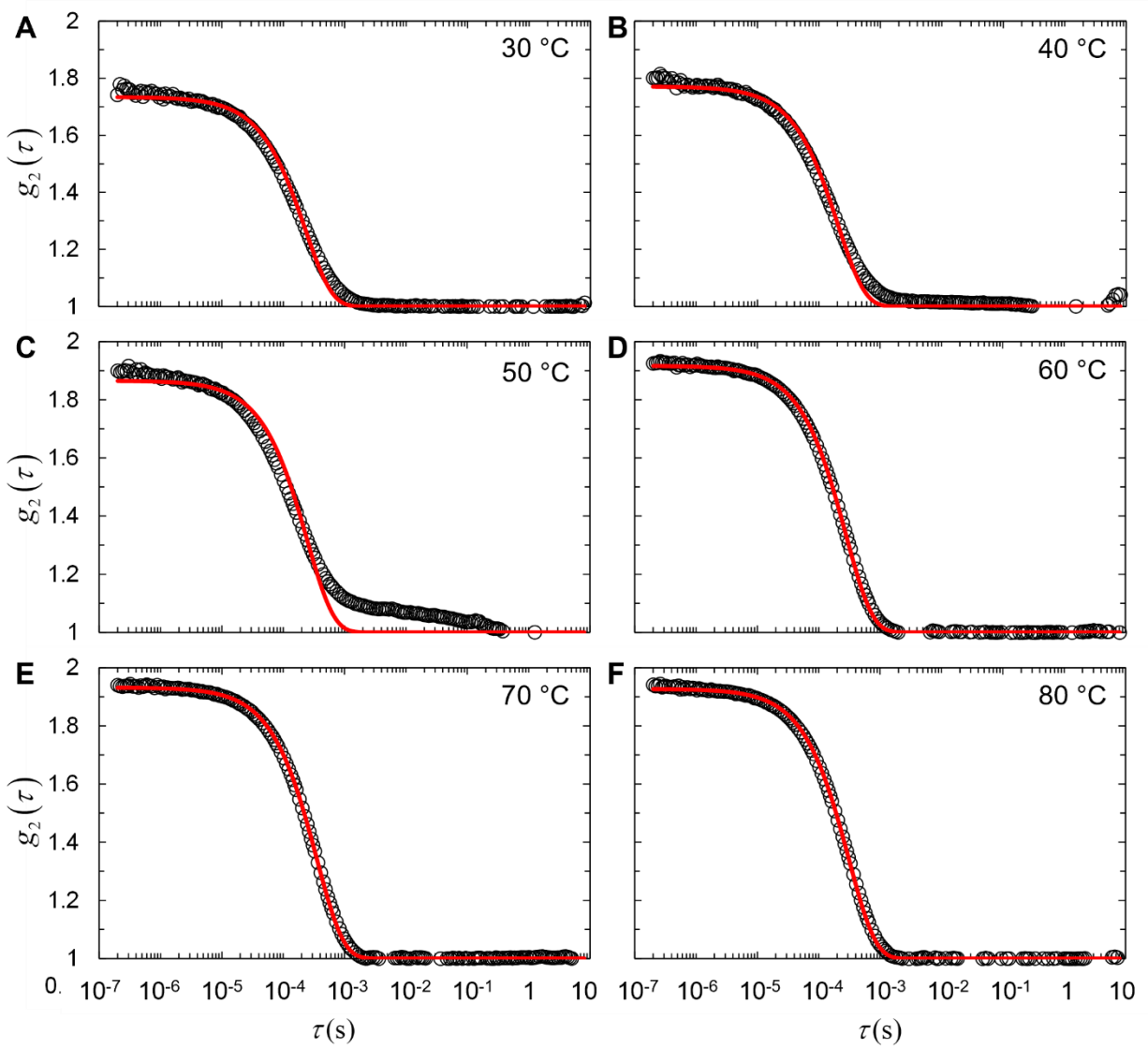

Temperature (°C)	30	40	50	60	70	80
a	0.734	0.771	0.865	0.917	0.931	0.927
Γ (s^{-1})	2187	2415	2047	1815	1417	1607

Figure S4. Autocorrelation function, $g_2(\tau) = \langle I(t) I(t+\tau) \rangle / \langle I(t) \rangle^2$, and the fitted exponential decay function, $1 + a \exp(-2\Gamma\tau)$, for 0.025 wt.% aqueous solution of MC (SM-4000) at (A) 30 °C, (B) 40 °C, (C) 50 °C, (D) 60 °C, (E) 70 °C, and (F) 80 °C. The empty circles show experimental data and the red line is the best fitted exponential decay function with the provided fitting parameters for each case.

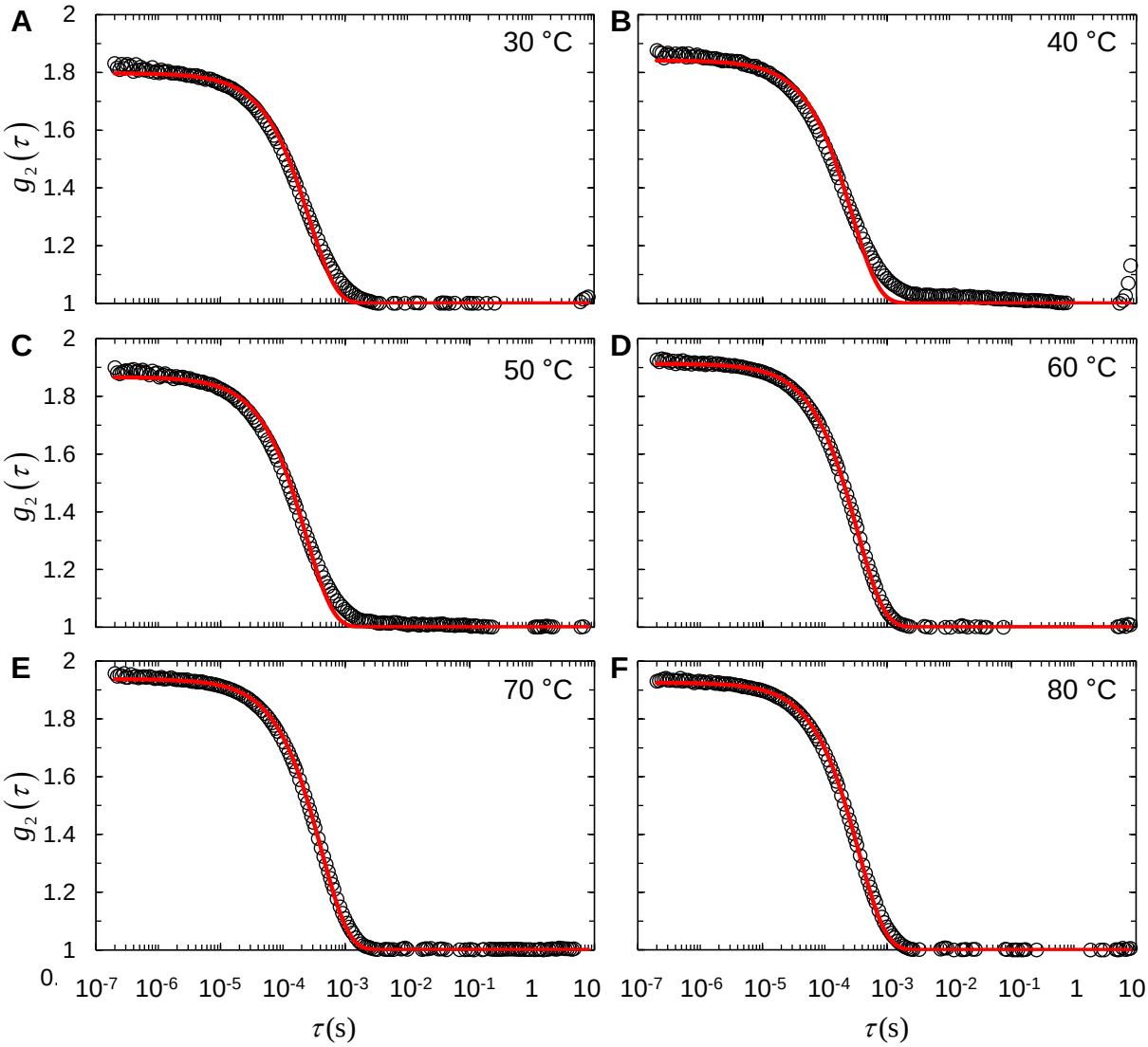

Temperature (°C)	30	40	50	60	70	80
a	0.797	0.842	0.866	0.913	0.937	0.926
Γ (s^{-1})	1877	1833	2124	1509	1205	1425

Figure S5. Autocorrelation function, $g_2(\tau) = \langle I(t) I(t+\tau) \rangle / \langle I(t) \rangle^2$, and the fitted exponential decay function, $1 + a \exp(-2\Gamma\tau)$, for 0.025 wt.% aqueous solution of MC (SM-8000) at (A) 30 °C, (B) 40 °C, (C) 50 °C, (D) 60 °C, (E) 70 °C, and (F) 80 °C. The empty circles show experimental data and the red line is the best fitted exponential decay function with the provided fitting parameters for each case.

Table S1. Estimates of overlap concentration, C^*, for different grades of HPC and MC.

Polymer	Trade name	MW (kg/mol)	N	R_g (nm)	C^* (wt.%)
HPC	HPC-SSL	40	68	12	0.42
	HPC-L	140	237	27	0.15
	HPC-M	700	1185	70	0.04
	HPC-H	1000	1693	86	0.03
	HPC-VH	2500	4232	150	0.02
MC	MC-25	85	225	26	0.10
	MC-100	150	398	36	0.07
	MC-400	200	530	43	0.05
	MC-4000	400	1060	65	0.03
	MC-8000	500	1326	75	0.03

MW for HPC and MC is reported in [9] and [10], respectively. Assuming a ~1 nm length (b) for the cellobiose, the R_g is estimated from $R_g \sim bN^{3/5}$ at room temperature,[7] where N is the number of monomer unit which is the quotient of MW divided by 590.8 g/mol and 377.2 g/mol—the monomer MW of HPC (with DS=2.3) and MC (with DS=1.9), respectively. Estimates for R_g are in agreement with earlier measurements.[11] As polymer solutions are dilute, we estimated the overlap concentration from $C^* = \mathrm{MW} / N_A (2R_g)^3$, where N_A is the Avogadro's number.[12]

References

1 C. Qian, S. J. Mumby and B. E. Eichinger, *Macromolecules*, 1991, **24**, 1655–1661.

2 A. J. Nedoma, M. L. Robertson, N. S. Wanakule and N. P. Balsara, *Macromolecules*, 2008, **41**, 5773–5779.

3 M. J. A. Hore, B. Hammouda, Y. Li and H. Cheng, *Macromolecules*, 2013, **46**, 7894–7901.

4 J. W. McAllister, P. W. Schmidt, K. D. Dorfman, T. P. Lodge and F. S. Bates, *Macromolecules*, 2015, **48**, 7205–7215.

5 F. Wang, P. Altschuh, L. Ratke, H. Zhang, M. Selzer and B. Nestler, *Advanced Materials*, 2019, **31**, 1806733.

6 T. Lindvig, M. L. Michelsen and G. M. Kontogeorgis, *Fluid Phase Equilibria*, 2002, **203**, 247–260.

7 M. Rubinstein and R. Colby, *Polymer Physics*, Oxford University Press, New York, United States, 2003.

8 J. Stetefeld, S. A. McKenna and T. R. Patel, *Biophysical Reviews*, 2016, **8**, 409–427.

9 M. Martin-Pastor and E. Stoyanov, *Journal of Polymer Science*, 2020, **58**, 1632–1641.

10 T. Kato, T. Tokuya and A. Takahashi, *Kobunshi Ronbunshu*, 1982, **39**, 293–298.

11 C. W. Hoogendam, A. de Keizer, M. A. Cohen Stuart, B. H. Bijsterbosch, J. A. M. Smit, J. A. P. P. van Dijk, P. M. van der Horst and J. G. Batelaan, *Macromolecules*, 1998, **31**, 6297–6309.

12 Qicong. Ying and Benjamin. Chu, *Macromolecules*, 1987, **20**, 362–366.